NASA CONTRACTOR REPORT

NASA CR-2123

NASA CR-2123

ASYMMETRIC HYPERSONIC FLOW

by Stephen H. Maslen

Prepared by
RESEARCH INSTITUTE FOR ADVANCED STUDIES
MARTIN MARIETTA CORPORATION
Baltimore, Md. 21227
for Langley Research Center

NATIONAL AERONAUTICS AND SPACE ADMINISTRATION • WASHINGTON, D. C. • SEPTEMBER 1972

1. Report No.	2. Government Accession No.	3. Recipient's Catalog No.
NASA CR-2123		

4. Title and Subtitle	5. Report Date
ASYMMETRIC HYPERSONIC FLOW	September 1972
	6. Performing Organization Code

7. Author(s)	8. Performing Organization Report No.
Stephen H. Maslen	
	10. Work Unit No.

9. Performing Organization Name and Address	11. Contract or Grant No.
Research Institute for Advanced Studies Martin Marietta Corporation 1450 S. Rolling Road Baltimore, Maryland 21227	NAS1-10193
	13. Type of Report and Period Covered
12. Sponsoring Agency Name and Address	Contractor Report
National Aeronautics and Space Administration Washington, D.C. 20546	14. Sponsoring Agency Code

15. Supplementary Notes

16. Abstract

A general method for the analysis of the inviscid asymmetric hypersonic flow fields enveloping smooth bodies of general shape is given. The method is based on the assumption of a thin shock layer which yields an explicit expression for pressure in generalized Mises coordinates. Numerical results for elliptic cones at angle of attack are shown to compare well with experiments and other theories. The computing logic for a blunt body is described, and a limiting solution at the stagnation point is presented.

17. Key Words (Suggested by Author(s))	18. Distribution Statement
Inviscid asymmetric hypersonic flow Thin shock layer	

19. Security Classif. (of this report)	20. Security Classif. (of this page)	21. No. of Pages	22. Price*
UNCLASSIFIED	Unclassified	33	$3.00

*For sale by the National Technical Information Service, Springfield, Virginia 22151

ASYMMETRIC HYPERSONIC FLOW

By S. H. Maslen
Research Institute for Advanced Studies
Martin Marietta Corporation

SUMMARY

A general method for the analysis of the inviscid asymmetric hypersonic flow fields enveloping smooth bodies of general shape is given. The method is based on the assumption of a thin shock layer which yields an explicit expression for pressure in generalized Mises coordinates. Numerical results for elliptic cones at angle of attack are shown to compare well with experiments and other theories. The computing logic for a blunt body is described, and a limiting solution at the stagnation point is presented.

INTRODUCTION

The supply of solutions for the inviscid flow in a shock layer, such as that about a blunted body moving at hypersonic speeds, is very large and it might appear that another such method would be, to say the least, superfluous. However the goals of this work are special. The aim is to find an efficient and economical solution for the shock layer in a three-dimensional geometry. An exact analysis is not sought but only a reliable one. Thus the precise time-dependent methods or even the method of characteristics are rejected because of the required computing time. On the other hand, Newtonian methods are simple but do not provide the desired detail in the shock layer.

Some time ago Maslen (ref. 1) proposed a method for axisymmetric flow based on the use of a Mises transformation coupled with a simple approximate integral of the lateral (to the shock) momentum equations. A number of solutions were given and the results were indeed accurate and very easy to obtain.

The simplicity of the method led several others to apply the method to elaborations of the original case. Jackson (ref. 2) considered viscous effects and also used the method to solve the complete equations of notion iteratively. Perini and Melnik (ref. 3) solved nonequilibrium flow, while Olstad (ref. 4) applied the procedure to radiating flow and to the massive blowing problem associated with extreme heating rates. Recently, Grose (ref. 5) has presented detailed solutions for nonequilibrium hypersonic flows for a variety of cases of interest in planetary entry.

The present analysis returns to the original inviscid equilibrium flow case, but we consider general three-dimensional geometry. None of the elaborations mentioned above will be examined herein. Indeed, the present work will be discussed for a perfect gas only. We do, however, attack the

direct problem (body given) although, as will be seen, the method is inverse and begins with a specified shock.

In addition to support of this work by NASA, grateful acknowledgement should be made for support, for several years, of particularly, the basic analysis, by the Mechanics Division of the Air Force Office of Scientific Research under contract F44620-69-C-0096.

Thanks are also due to Carl Hutton who carried out much of the computer programming.

SYMBOLS

a	square root of nose radius of curvature, eq. (64)
A	auxiliary function, eq. (7) or eq. (67a)
B	auxiliary function, eq. (7) or eq. (64)
D	auxiliary function, eq. (7)
E	auxiliary function, eq. (7)
G, H	functions defined in eq. (69)
h	enthalpy
K	longitudinal shock curvature, eq. (35a)
L	differential operator, eq. (9)
$\bar{L}$	differential operator, eq. (37b)
m	auxiliary angle, eq. (59a)
M_∞	free stream Mach number
P	pressure
P_1, P_2	pressure functions, eq. (54), (55)
r	cylindrical radius
S	"entropy"
u_1, v_1, w_1	velocity components, cylindrical coordinates
U, V, W	velocity components, defined in eqs. (4)
$\bar{V}$	$\sqrt{V^2 + W^2}$
x, r, ω	cylindrical coordinates, fig. 1

x_1, r_1, w_1 cylindrical coordinates (wind axes)

z shock layer coordinate, fig. 1, and eq. (2)

α angle of attack

β auxiliary function, eq. (23)

γ ratio of specific heats

Δ auxiliary function, eq. (7)

η shock layer coordinate, fig. 1 and eq. (2)

ζ "Mises" type coordinate, eq. (8)

$\bar{\zeta}$ coordinate used in stagnation point analysis, eq. (72)

θ shock layer coordinate, fig. 1 and eq. (2)

λ $\mathrm{Tan}^{-1}\left(\frac{1}{r}\,\partial r/\partial\theta\right)_s$, fig. 1

ν $\mathrm{Tan}^{-1}\left(\partial r/\partial z\right)_s$, fig. 1

ξ $\mathrm{Tan}^{-1}\,(W/V)$

ρ density

σ "Mises" type coordinate, eq. (8)

$\bar{\sigma}$ coordinate used in stagnation point analysis, eq. (72)

τ $\mathrm{Tan}^{-1}\,(\mathrm{Tan}\,\nu\,\mathrm{Cos}\,\lambda)$, fig. 1

φ stream function, eq. (5)

ψ stream function, eq. (5), also "Mises" type coordinate, eq. (8)

$\bar{\psi}$ conical variable, eq. (37a)

Subscripts:

s shock value

∞ free stream value

o stagnation line shock value

$x,\ r,\ \omega$

$z,\ \eta,\ \theta$

$\zeta,\ \sigma,\ \psi$

$\bar{\zeta},\ \bar{\sigma}$

} partial derivative

GENERAL ANALYSIS

Differential Equations

We start with the equations of motion for steady, inviscid, isoenergetic flow, written in cylindrical coordinates $(x,\ r,\ \omega)$, with corresponding velocities u_1, v_1 and w_1. It is important to keep track of the coordinates as two other systems will be used at various points in the analysis. One has, using subscripts for differentiation,

$$(\rho u_1)_x + \frac{1}{r}(r\rho v_1)_r + \frac{1}{r}(\rho w_1)_\omega = 0 \tag{1a}$$

$$\rho(u_1 u_{1x} + v_1 u_{1r} + \frac{1}{r} w_1 u_{1\omega}) = -P_x \tag{1b}$$

$$\rho(u_1 v_{1x} + v_1 v_{1r} + \frac{1}{r} w_1 v_{1\omega} - \frac{w_1^2}{r}) = -P_r \tag{1c}$$

$$\rho(u_1 w_{1x} + v_1 w_{1r} + \frac{w_1 w_{1\omega}}{r} + \frac{v_1 w_1}{r}) = -\frac{P_\omega}{r} \tag{1d}$$

$$(u_1 \frac{\partial}{\partial x} + v_1 \frac{\partial}{\partial r} + \frac{w_1}{r} \frac{\partial}{\partial w})\ (S) = 0 \tag{1e}$$

$$S = S(P,\ \rho) \tag{1f}$$

where S is related to the entropy and where one of the momentum equations can be replaced conveniently by the isoenergetic condition,

$$h + (u_1^2 + v_1^2 + w_1^2)/2 = \text{constant} \tag{1g}$$

Now consider a second set of coordinates related to the flow geometry (Fig. 1). We base them on the shock and define $z,\ \eta,\ \theta$ where $z,\ \theta$ are the axial and azimuthal coordinates of a point on the shock while η is the (normal) distance from shock to field point $(x,\ r,\ \omega)$. The two coordinate systems are related by

$$x = z + \eta \text{ Sin } \tau$$

$$r^2 = r_s^2 + \eta^2 \text{ Cos}^2 \tau - 2\eta r_s \text{ Cos } \tau \text{ Cos } \lambda \tag{2}$$

$$r \text{ Sin } (\omega-\theta) = \eta \text{ Cos } \tau \text{ Sin } \lambda$$

where $r_s = r_s(z,\theta)$ is the equation of the shock

$$\text{Tan } \nu = (\partial r_s/\partial z)$$

$$\text{Tan } \lambda = \frac{1}{r}(\partial r_s/\partial \theta) \tag{3}$$

$$\text{Tan } \tau = \text{Tan } \nu \text{ Cos } \lambda$$

Note that from eqs. (3) we have

$$\frac{\partial \tau}{\partial \theta} + \text{Sin } \tau \text{ Cos } \tau \text{ Tan } \lambda \left(\frac{\partial \lambda}{\partial \theta} - 1 \right) = \frac{r_s \text{ Cos}^2 \tau}{\text{Cos } \lambda} \frac{\partial \lambda}{\partial z} \tag{3a}$$

Now introduce three mutually perpendicular velocity components, U, V, W where U is normal to the shock and V, W are otherwise arbitrarily chosen. Then

$$U = u_1 \text{ Sin } \tau - v_1 \text{ Cos } \tau \text{ Cos } (\omega-\theta+\lambda) + w_1 \text{ Cos } \tau \text{ Sin } (\omega-\theta+\lambda)$$

$$V = u_1 \text{ Cos } \tau + v_1 \text{ Sin } \tau \text{ Cos } (\omega-\theta+\lambda) - w_1 \text{ Sin } \tau \text{ Sin } (\omega-\theta+\lambda) \tag{4}$$

$$W = \qquad - v_1 \text{ Sin } (\omega-\theta+\lambda) \qquad - w_1 \text{ Cos } (\omega-\theta+\lambda)$$

Equation (1a) can be solved by the introduction of a pair of stream functions, ψ and φ, such that

$$\rho \vec{U} = \vec{\nabla}\psi \times \vec{\nabla}\varphi \tag{5}$$

or

$$\rho r U = (\psi_z \varphi_\theta - \psi_\theta \varphi_z)/\Delta$$

$$\rho(DV + EW) = \psi_\eta \varphi_z - \varphi_\eta \psi_z \tag{6}$$

$$\rho(AV + BW) = \frac{1}{r}(\psi_\theta \varphi_\eta - \psi_\eta \varphi_\theta)$$

where A, B, D, E and Δ are geometric factors given by

$$A = [r_s + \eta \cos\tau \cos\lambda (\lambda_\theta - 1)]/r \cos\lambda$$

$$B = \frac{\eta}{r} \tau_\theta$$

$$D = \tan\tau \tan\lambda + \eta\lambda_z \cos\tau \tag{7}$$

$$E = (1 + \eta\tau_z \cos\tau)/\cos\tau$$

$$\Delta = AE - BD$$

Now introduce a final coordinate system. This is a sort of Mises transformation in which we interchange ψ and η as dependent and independent variables. The specific use will clearly depend on the way in which ψ and φ (eq. (5)) are subsequently chosen. Let the new independent variables be ψ, ζ, σ

where

$$\zeta = z$$

$$\sigma = \theta \tag{8}$$

$$\psi = \psi(\eta, z, \theta)$$

Further, define the operator L by

$$\bar{V}L = -\frac{(DV + EW)}{r}\frac{\partial}{\partial\sigma} + (AV + BW)\frac{\partial}{\partial\zeta} \tag{9}$$

where

$$\bar{V}^2 = V^2 + W^2 \tag{9a}$$

Then equations (6) yield, noting (7)

$$L(\varphi) = 0 \tag{10}$$

$$\bar{V}L(\eta) = U\Delta \tag{11}$$

$$\rho\eta_\psi = \frac{-\varphi_\sigma}{r(AV + BW)} = \frac{-\varphi_\zeta}{DV + EW} \tag{12}$$

The energy equation (1a) becomes

$$L(S) = 0 \tag{13}$$

while the isoenergetic condition (1f) is

$$h + \frac{1}{2}(U^2 + V^2 + W^2) = \text{constant} \tag{14}$$

The momentum equations, only two of which are required, become

$$-\Delta \frac{P_\psi}{\eta_\psi} = \rho\bar{V}\,[L(U) - VL(\tau) + W\,\mathrm{Cos}\,\tau\; L(\lambda-\theta)] \tag{15}$$

$$-[A(P_\zeta - P_\psi\,\eta_\zeta/\eta_\psi) - \frac{D}{r}(P_\sigma - P_\psi\,\eta_\sigma/\eta_\psi)]$$
$$= \rho\bar{V}\,[L(V) + UL(\tau) - W\,\mathrm{Sin}\,\tau\; L(\lambda-\theta)] \tag{16}$$

$$-[B(P_\zeta - P_\psi\,\eta_\zeta/\eta_\psi) - \frac{E}{r}(P_\sigma - P_\psi\,\eta_\sigma/\eta_\psi)]$$
$$= \rho\bar{V}\,[L(W) + (V\,\mathrm{Sin}\,\tau - U\,\mathrm{Cos}\,\tau)\,L(\lambda-\theta)] \tag{17}$$

These last three equations can be combined to give the Bernoulli relation

$$L(P) = \frac{\rho}{2} L(U^2 + V^2 + W^2) = 0 \tag{18}$$

The equations to be solved then consist of (10), (11), (12), (13), (14), any two of (15)-(18) and a state relation. The dependent variables are the three velocity components (U, V, W), the thermodynamic variables (P, ρ, S, h), one physical coordinate (η), and one stream function (φ).

For later use, we will need the values of P_ψ at the shock. After some labor

$$\frac{P_\psi}{\rho\eta_\psi} = \mathrm{Cos}\,\tau\;\mathrm{Cos}\,\lambda\,[\bar{V}VL(\tau) - \bar{V}W\mathrm{Cos}\,\tau\; L(\lambda-\theta)]\left\{\frac{1 - \dfrac{dU}{U_\infty d\mathrm{Sin}\,\beta} + \dfrac{U}{\rho U_\infty c^2}\dfrac{dP}{d\mathrm{Sin}\,\beta}}{1 - U^2/c^2}\right\}$$
$$-\frac{\rho U^2}{\rho_\infty}\left[\tau_z\,\mathrm{Cos}\,\tau - \frac{\mathrm{Cos}\,\tau\;\mathrm{Cos}\,\lambda}{r}(1-\lambda_\theta) - \frac{\mathrm{Sin}\,\tau\;\mathrm{Sin}\,\lambda\;\tau_\theta}{r}\right]\left\{\frac{1 - \rho_\infty/\rho}{1 - U^2/c^2}\right\} \tag{19}$$

where c is the speed of sound behind the shock. Note that all the derivatives on the right side lie along the shock since, clearly, ζ and σ in the operator L as used here can be replaced by z, θ.

Boundary Conditions

Consider that the free stream is a uniform flow (ρ_{∞}, U_{∞}, etc.) at an angle of attack α(Fig. 1) with respect to the x (or z) axis. If (x_1, r_1, ω_1) are cylindrical coordinates in the wind system,

$$x_1 = x \text{ Cos } \alpha + r \text{ Sin } \omega \text{ Sin } \alpha$$

$$r_1 \text{ Cos } \omega_1 = r \text{ Cos } \omega \tag{20}$$

$$r_1 \text{ Sin } \omega_1 = r \text{ Sin } \omega \text{ Cos } \alpha - x \text{ Sin } \alpha$$

Then, in the free stream, we can set

$$\varphi = \omega_1 = \text{Tan}^{-1}\left[\frac{r \text{ Sin}\omega \text{ Cos } \alpha - x \text{ Sin } \alpha}{r \text{ Cos } \omega}\right] \tag{21}$$

$$\psi = \frac{\rho_{\infty}U_{\infty}r_1^2}{2} = \frac{\rho_{\infty}U_{\infty}}{2}\left[(r \text{ Cos}\omega)^2 + (r \text{ Sin } \omega \text{ Cos } \alpha - x \text{ Sin } \alpha)^2\right]$$

$$\equiv \frac{\rho_{\infty}U_{\infty}}{2}\left[\frac{r \text{ Cos } \omega}{\text{Cos } \varphi}\right]^2 \tag{22}$$

Equations (21) and (22) are consistent with eq. (5) in the uniform free stream and, for axial symmetry, ψ is simply the usual Stokes stream function. The shock is taken to be Rankine-Hugoniot. The quantities ρU, V, W, φ, ψ and $\rho\eta_{\psi}$ are continuous across it. Thus, immediately behind the shock

$$\rho U/\rho_{\infty}U_{\infty} = \text{Sin } \tau \text{ Cos } \alpha - \text{Cos } \tau \text{ Sin } \alpha \text{ Sin } (\theta-\lambda) \equiv \text{Sin } \beta \tag{23}$$

$$V/U_{\infty} = \text{Cos } \tau \text{ Cos } \alpha + \text{Sin } \tau \text{ Sin } \alpha \text{ Sin } (\theta-\lambda) \tag{24}$$

$$W/U_{\infty} = - \text{Sin } \alpha \text{ Cos } (\theta-\lambda) \tag{25}$$

$$\varphi = \mathrm{Tan}^{-1}\left[\frac{r_s \sin\theta \cos\alpha - z \sin\alpha}{r_s \cos\theta}\right] \tag{26}$$

$$1/\eta_\psi = \rho U_\infty \{z(\sin\tau - \cos\alpha \sin\beta) - r(\cos\tau \cos\lambda + \sin\theta \sin\alpha \sin\beta)\} \tag{27}$$

where $\sin\beta$ is defined by eq. (23). Clearly, $(\pi/2-\beta)$ is the angle between the wind direction and the normal to the shock so that the Mach number normal to the shock is $M_\infty \sin\beta$. The Rankine Hugoniot relations yield

$$P/P_\infty = 1 + \gamma M_\infty^2 \sin^2\beta\,(1 - \rho_\infty/\rho) \qquad \text{(shock)} \tag{28}$$

where, for a perfect gas

$$\rho/\rho_\infty = \frac{\gamma+1}{2}(M_\infty \sin\beta)^2 \Big/ \left[1 + \frac{\gamma-1}{2}(M_\infty \sin\beta)^2\right] \qquad \text{(shock)} \tag{29}$$

At the body surface, we would like to have $\psi = 0$. This requires (see eqs. (22) and (20)) that the origin of coordinates be chosen so that $r_1 = 0$ occur on the stagnation streamline. If this selection can be made, there is no further worry about body surface conditions.

Special Cases

For convenience, the special limiting cases of axial symmetry and general conical flow will be recorded.

Axial Symmetry

For this case $W = w_1 = \lambda = \partial/\partial\theta = \partial/\partial\omega = \partial/\partial\sigma = 0$ and $\varphi = \sigma$, $\tau = \nu$. Then, successively, from eqs. (13), (12), (11), (14) and (15), there follows

$$S = S(\psi) \tag{30}$$

$$\eta_\psi = -1/r\rho V \tag{31}$$

$$U = \frac{V\eta_\zeta}{E} \tag{32}$$

$$h + \frac{U^2 + V^2}{2} = \text{const.} \tag{33}$$

$$P_{\psi} = \frac{U_{\zeta} - V\tau_z}{rE} \tag{34}$$

where, from eqs. (7) and (2)

$$\begin{aligned} E &= (1 + \eta \cos\tau\ \tau_z)/\cos\tau \\ r &= r_s(z) - \eta \cos\tau \end{aligned} \tag{35}$$

Note that the shock curvature, K(z) is given by

$$K(z) = -\tau_z \cos\tau \tag{35a}$$

The boundary conditions at the shock (see eqs. (22)-(29)) become

$$\begin{aligned} \rho U/\rho_{oo} U_{oo} &= \sin\tau \\ V/U_{oo} &= \cos\tau \\ 1/\eta_{\psi} &= -\rho U_{oo} r \cos\tau \\ \psi &= \frac{\rho_{oo} U_{oo}}{2} r^2 \end{aligned} \tag{36}$$

and, in eqs, (28) and (29), we replace β with τ (or ν).

Conical flow

For this case, $r_s = z \tan\nu\ (\theta)$ so that $\lambda_z = \tau_z = 0$. Further, all the physical quantities (plus η/z) depend only on σ. Define

$$\bar{\psi} = \psi/\zeta^2 \tag{37a}$$

and the operator $\bar{L}$ by

$$\bar{V}\bar{L} \equiv -\bar{V}_\zeta L = \frac{(DV + EW)}{\text{Tan } \nu} \frac{\partial}{\partial \sigma} + 2\bar{\psi}(AV + BW) \frac{\partial}{\partial \psi} \tag{37b}$$

Then eqs. (12), (11), (13), (10), (14) become

$$\rho \frac{\partial(\eta/z)}{\partial \bar{\psi}} = \frac{-\varphi_\sigma}{\text{Tan } \nu \ (AV + BW)} \tag{38}$$

or

$$\eta/z = \frac{\text{Cos } \lambda}{\text{Tan } \nu} \int_{\bar{\psi}}^{\bar{\psi}_s} \frac{\varphi_\sigma d\bar{\psi}}{\rho \left[V + \eta \frac{\text{Cos } \tau}{z \text{ Tan } \nu} \text{Cos } \lambda \ (\lambda_\theta - 1) \ (V - W \text{ Sin } \tau \text{ Tan } \lambda)\right]} \tag{38a}$$

and

$$VL \ (\eta/z) = -U_\Delta - \frac{\eta}{z} (AV + BW) \tag{39}$$

$$\bar{L}(S) = 0 \tag{40}$$

$$\bar{L}(\varphi) = 0 \tag{41}$$

$$h + \frac{1}{2} (U^2 + \bar{V}^2) = \text{constant} \tag{42}$$

And in eqs. (15), (16) and (17) we replace L, P_ψ, P_ζ, η_φ, η_σ and η_ζ as follows

$$\begin{aligned} L &\to \bar{L} \\ P_\psi &\to P_{\bar{\psi}} \\ P_\zeta &\to -2\bar{\psi} P_{\bar{\psi}} \\ \eta_\psi &\to (\eta/z)_{\bar{\psi}} \\ \eta_\sigma &\to (\eta/z)_\sigma \\ \eta_\zeta &\to -2\bar{\psi}(\eta/z)_{\bar{\psi}} - (\eta/z) \end{aligned} \tag{43}$$

The boundary conditions at the shock (eqs. (22)-(29)) are unchanged except that the left side of eqs. (27) becomes

$$z/(\eta/z)_{\bar{\psi}}$$

while, at the shock eq. (22) is replaced by

$$\bar{\psi} = \frac{\rho_\infty U_\infty}{2}\left(\frac{r \cos \omega}{z \cos \varphi}\right)^2 \tag{44}$$

APPROXIMATIONS

The system described thus far is complete and can be solved if one works hard enough. However, the object is to provide a reasonably accurate method of solution which is at the same time simple. We will depend on the shock layer geometry to provide that simplification. It is clear that, except very near the stagnation point, the velocity normal to the shock ($\bar{U}$) will be much less than that parallel to it ($\bar{V}$ or V, W). Also, as discussed in reference 1, the pressure gradient normal to the shock (or P_ψ) is well approximated by using, throughout the shock layer, its value at the shock, again neglecting U. This last approximation is most valid for blunt body geometry (as opposed to conical; more on that later) where the majority of the mass flow tends to be thrown toward the shock with low density near the body.

The system which results is illustrated most conveniently for the axial symmetry case. One has, successively, from eqs. (34), (30), (33), (31), using (35) (the subscript s refers to conditions at the shock)

$$P_\psi = -\left(\frac{V^\tau \zeta}{r_s \bar{E}}\right)_s = \left(\frac{KV}{r}\right)_s \tag{45}$$

or

$$P(\psi,\zeta) = P_s(\zeta) + \left(\frac{KV}{r}\right)_s (\psi - \psi_s(\zeta)) \tag{46}$$

and

$$S = S(\psi) \tag{47}$$

$$h = h(P,S), \rho = \rho\ (P,S) \qquad \text{(state)} \tag{48}$$

$$\bar{V}^2 = a(\text{const} - h) \tag{49}$$

$$\eta_\psi = -\frac{1}{r\rho V} \tag{50}$$

$$r^2 = r_s^2(\zeta) - 2V_s\int_\psi^{\psi_s(\zeta)} \frac{d\psi}{\rho V} \tag{51}$$

For a given shock, the equations can be solved successively in a straightforward manner. Because the procedure is so simple, the direct (body given) problem is readily solved by iteration. Excellent results are illustrated in ref. (1) for this axisymmetric case. It should be noted (see Jackson (ref. 2)) that this solution forms a basis for an iterative solution of the complete system although such is not intended here.

As is shown in ref. (1), for the stagnation point and for the surface of a circular cone, eq. (46) indicates that the pressure is the same as that at the shock. Iteration of the equations by using the results of this simple solution to evaluate the omitted terms in the exact equations corrects this result very nicely. It would be desirable to incorporate in the original solution a form allowing such corrections for these cases. Such a result is found by starting with the form given in eq. (19). However, we set the terms in curly brackets equal to unity. Then, using eq. (27),

$$P_\psi = \left[\text{Cos}\,\tau\ (V^2\tau_z) - \frac{\rho U^2}{\rho_\infty}\left(\text{Cos}\,\tau\ \tau_z - \frac{\text{Cos}\,\tau}{r}\right)\right]\left(-\frac{1}{U_\infty r\,\text{Cos}\,\tau}\right)$$

$$= -\left(\frac{V^2\tau_z}{rU_\infty}\right)_s - \left[\frac{\rho U^2}{r\rho_\infty U_\infty}\left(\frac{1}{r} - \tau_z\right)\right]_s$$

If we assume that the second term should actually be proportional to ψ (i.e., multiplied by ψ/ψ_s) we get

$$P(\psi_\zeta,\zeta) = P_s(\zeta) + \left(\frac{KV\psi}{r}\right)_s \frac{(\psi - \psi_s(\zeta))}{\psi_s(\zeta)} - \left[\psi\,\frac{U\text{Tan}\,\tau}{r}\left(K + \frac{\text{Cos}\,\tau}{r}\right)\right]_\zeta \frac{(\psi^2 - \psi_s^2(\zeta))}{2\psi_s^2(\zeta)} \tag{52}$$

At the stagnation point, taking limiting values, we find

$$\frac{P(\psi,\zeta)}{\rho_\infty U_\infty^2} = \frac{P_s(0)}{\rho_\infty U_\infty^2} + \frac{\rho_\infty}{2\rho}\left[1 - \frac{\psi^2}{\psi_s^2}\right] \tag{52a}$$

For a cone (K = 0) we get

$$\frac{P(\psi,\zeta)}{\rho_\infty U_\infty^2} = \frac{P_s}{\rho_\infty U_\infty^2} + \frac{\rho_\infty}{4\rho}\,\mathrm{Sin}^2\,\tau\left[1 - \frac{\psi^2}{\psi_s^2}\right] \tag{52b}$$

These are accurate solutions for the pressure, particularly the surface pressure, for the two cases.

This rather tortuous path to an expression for the pressure has been followed to provide some rationale for the final form to be used in the general case. It is clear that the justification for more complexity than the simple expression in eq. (46) lies largely in experience with its application. However one can observe the following. The second term in eq. (19) is very largely $\rho UU_\psi/\rho\eta_\psi$ and represents the recompression tendency across the shock layer due to curvature of the streamlines from their direction at the shock to lie along the body. This effect is largest at the shock and falls toward the body; the simplest assumption is that it is proportional to ψ. Such a variation is consistent with eqs. (52).

With these preliminaries, we can now describe the procedure to be followed in general. We treat eqs. (19) and (27) as before and write

$$P(\psi,\zeta,\sigma) = P_s(\zeta,\sigma) + P_1(\zeta,\sigma)(\psi - \psi_s) - P_2(\zeta,\sigma)\left(\frac{\psi^2 - \psi_s^2}{2\psi_s}\right) \tag{53}$$

where

$$P_1 = \left\{\frac{\mathrm{Cos}\,\tau\,\mathrm{Cos}\,\lambda\,[\bar{V}VL(\tau) - \bar{V}W\mathrm{Cos}\,\tau\,L(\lambda-\theta)]}{\rho U_\infty\,[z(\mathrm{Sin}\,\tau - \mathrm{Cos}\,\alpha\,\mathrm{Sin}\,\beta) - r(\mathrm{Cos}\,\tau\,\mathrm{Cos}\,\lambda + \mathrm{Sin}\,\theta\,\mathrm{Sin}\,\alpha\,\mathrm{Sin}\,\beta)]}\right\}_s \tag{54}$$

and

$$P_2 = \left\{\frac{\rho U^2\,[\mathrm{Cos}\,\tau\,\tau_z - \mathrm{Cos}\,\tau\,\mathrm{Cos}\,\lambda\,(1-\lambda_\theta)/r - \mathrm{Sin}\,\tau\,\mathrm{Sin}\,\lambda\,\tau_\theta/r]}{\rho_\infty U_\infty[z(\mathrm{Sin}\,\tau - \mathrm{Cos}\,\alpha\,\mathrm{Sin}\,\beta) - r(\mathrm{Cos}\,\tau\,\mathrm{Cos}\,\lambda + \mathrm{Sin}\,\theta\,\mathrm{Sin}\,\alpha\,\mathrm{Sin}\,\beta)]}\right\}_s \tag{55}$$

Before leaving the subject of the pressure distribution, it is worth remarking that the exact form of eq. (53) has no effect on the logic of the program provided only that the relation is an explicit one when the shock is known. The particular form used in ref. (1) (eq. (46)) is equivalent to setting P_2 equal to zero in eq. (53). That or the complete form given in eq. (53) (or, for that matter, other alternatives) are really to be evaluated in the light of experience with the computer programs for the general problem; which programs are not yet operational.

Finally, eq. (14) becomes

$$h + \frac{\bar{V}^2}{2} = \text{constant} \tag{56}$$

while equations (9), (10) and (13) are applied, but setting $\eta = 0$ in A, B, D, E. Thus we have

$$\begin{aligned} A &= 1/\text{Cos } \lambda \\ B &= 0 \\ D &= \text{Tan } \tau \text{ Tan } \lambda \\ E &= 1/\text{Cos } \tau \end{aligned} \tag{57}$$

Finally we define an angle ξ by

$$\begin{aligned} V &= \bar{V}\text{Cos } \xi \\ W &= \bar{V}\text{Sin } \xi \end{aligned}$$

Then neglecting u and η, the two momentum equations (16) and (17) can be combined to yield

$$\rho\bar{V}^2 [L(\xi) + \text{Sin } \tau \; L(\lambda - \theta)] = A \text{ Sin } \xi \; P_\zeta + (E \text{ Cos } \xi - D \text{ Sin } \xi) \frac{P_\sigma}{r} \tag{58}$$

Equations (53), (56), (9), (10), (13) and (58) plus a state equation are a system of six equations for P, ρ, h, S, φ, $\bar{V}$ and ξ. The only differential operator appearing is L (eq. (9)) which is the ordinary derivative along a streamline.

For conical flow, a convenient alternate to eq. (58) is found by observing that (exactly) $\zeta P_\zeta + \eta P_\eta = 0$, so that eqs. (16) and (17) yield, neglecting η and U,

$$L\left[\tilde{V}\ \mathrm{Cos}\ (\xi + m)\right] = \frac{\tilde{V}^2\ \mathrm{Cos}\ \nu\ \mathrm{Sin}^2\ (\xi + m)}{\mathrm{Cos}\ \tau\ \mathrm{Cos}\ \lambda} \qquad \text{(conical)} \tag{59}$$

where
$$\mathrm{Tan}\ m = \mathrm{Sin}\ \tau\ \mathrm{Tan}\ \lambda \tag{59a}$$

After the system is solved, the solution is completed by returning to the physical (z, θ, η) space via eq. (12). Experience in the axisymmetric case has shown that it is preferable to evaluate eq. (12) exactly without making the small η approximation of eqs. (57).

Finally, from eq. (9), the equation for the streamlines is

$$\frac{d\sigma}{d\zeta} = \frac{-(DV + EW)}{r(AV + BW)} \tag{60}$$

while along the streamlines, eq. (58) becomes

$$\begin{aligned}\frac{d\ \mathrm{Sin}\ \xi}{d\zeta} = \frac{1}{\rho \tilde{V}^2}\Bigg\{&\mathrm{Sin}\ \xi\left(P_\zeta - \frac{\mathrm{Tan}\ \tau\ \mathrm{Sin}\ \lambda}{r}\ P_\sigma\right) + \frac{\mathrm{Cos}\ \xi\ \mathrm{Cos}\ \lambda}{r\ \mathrm{Cos}\ \tau}\ P_\sigma\Bigg\} \\ &+ \mathrm{Sin}\ \xi\left[\frac{\mathrm{Cos}\ \lambda\ \mathrm{Tan}\ \tau\ (\lambda_\theta - 1)}{r}\right] - \frac{\mathrm{Cos}\ \xi\ \mathrm{Cos}\ \lambda\ \mathrm{Tan}\ \tau}{r\ \mathrm{Cos}\ \tau}\,\tau_\theta\end{aligned} \tag{61}$$

We proceed by assuming a shock. The pressure is then explicitly given by eq. (53). We then find the position of each streamline. On each, φ and the entropy, S, are constant. Thus for a given point in the ψ, ζ, σ space the pressure is known and if the point lies on a specified streamline, then S, ψ, h, ρ and $\tilde{V}$ are known. Equations (60) and (61) can be solved for ξ and the streamline shape.

For conical flow, equations (60), (61) are written (using eqs. (37a) (59) and (57))

$$2\bar{\psi}\ \frac{d\sigma}{d\bar{\psi}} = \frac{(DV + EW)}{\mathrm{Tan}\ \nu\ (AV + BW)} = \frac{\mathrm{Cos}\ \lambda\ \mathrm{Sin}\ (\xi + m)}{\mathrm{Sin}\ \nu\ \mathrm{Cos}\ \xi} \qquad \text{Conical} \tag{62}$$

$$2\bar{\psi}\,\frac{d\,[\bar{V}\,\mathrm{Sin}\,(\xi+m)]}{d\bar{\psi}} = \frac{-\bar{V}^2\mathrm{Cos}\,\nu\,\mathrm{Sin}^2\,(\xi+m)}{\mathrm{Cos}\,\tau\,\mathrm{Cos}\,\lambda} \tag{63}$$

STAGNATION LINE

It is clear that the approximations employed to permit a convenient solution are not really valid in the stagnation region. However, as shown in ref. (1) for the axially symmetric case, the model yields a good shock standoff value. In the present case where an unsymmetric stagnation region is contemplated, the requirement is more severe. Not only do we need a reasonable standoff value, but it should turn out not to depend on the direction from which the stagnation line is approached. We examine this point next.

Consider the case corresponding to the first approximation (eq. (46)) for the pressure distribution. Without loss, set $\alpha = 0$. Near the stagnation line, the equation of the shock must be of the form

$$r^2 = 2a^2(\theta)z \tag{64a}$$

where the radius of curvature is given by (normalizing everything with respect to the radius of curvature at $\theta = \pi/2$)

$$a^2(\theta) = (1 + B\,\mathrm{Cos}^2\theta)^{-1} \tag{64b}$$

After some labor it follows that in the limit as $z \to 0$, eq. (54) gives

$$P_1 = \frac{u_{oo}}{(a^2\mathrm{Cos}\,\lambda)^2}\left[1 + \frac{\mathrm{Tan}\,\lambda\,(a^2\mathrm{Cos}\,\lambda)_\theta}{a^2\mathrm{Cos}\,\lambda}\right] \tag{65}$$

where
$$a^2\mathrm{Cos}\,\lambda = (1 + 2B\,\mathrm{Cos}^2\theta + B^2\mathrm{Cos}^2\theta)^{-1} \tag{66}$$

also
$$u_s = u_{oo}\,\mathrm{Sin}\,\tau$$

$$v_s = M_{oo}\,\mathrm{Cos}\,\tau$$

$$\psi_s = a^2 z(\rho_{oo}u_{oo})$$

$$\mathrm{Cos}\,\tau = \sqrt{2z}/(a\,\mathrm{Cos}\,\lambda)$$

and for a perfect gas

$$\frac{P_s(z,\theta)}{\rho_\infty U_\infty^2} = \left[\frac{2}{\gamma+1} - \frac{\gamma-1}{\gamma(\gamma+1)M_\infty^2}\right] - \frac{2\,\mathrm{Cos}^2\tau}{\gamma+1} \tag{67a}$$

$$= A - \frac{B}{2}\left[\mathrm{Cos}^2\tau - 2z/(a^2\,\mathrm{Cos}^2\lambda)\right]$$

Then

$$P_s(\psi,\varphi) = A - \frac{B}{2}\left[\frac{2\psi}{\rho_\infty U_\infty (a^2(\varphi)\ \mathrm{Cos}\ \lambda\ (\varphi))^2}\right]$$

so that

$$\frac{P(z,\theta)}{\rho_\infty U_\infty^2} = A - \frac{B}{2}\,\mathrm{Cos}^2\tau + \frac{P_1}{U_\infty}\left[\frac{\psi}{\rho_\infty U_\infty} - a^2 z\right] \tag{67b}$$

Meanwhile, for a perfect gas

$$h = \frac{\gamma}{\gamma-1}\,P/\rho$$

$$\bar{V}^2 = \bar{V}_s^2\ (\varphi,\psi) + 2(h_s - h)$$

$$\bar{V}^2 = \frac{\rho_\infty U_\infty^2}{\rho_o}\left\{2zG(\theta)a^2 + \frac{2\psi}{\rho_\infty U_\infty}\left[H(\varphi) - \frac{P_1(\theta)}{U_\infty}\right]\right\} \tag{68}$$

$$\frac{P_\sigma}{\rho_\infty U_\infty^2} = \frac{P_{1\theta}(\psi)}{\rho_\infty U_\infty^2} - 2a^2 zG(\theta)\,\mathrm{Tan}\ \lambda$$

$$\frac{P_z}{\rho_\infty U_\infty^2} = -\,a^2 G(\theta)$$

where

$$G(\theta) = \frac{\rho_{oo} P_1(\theta)}{\rho_o U_{oo}} + B/(a^2 \text{Cos } \lambda)^2$$

$$H(\varphi) = [\rho_o/\rho_{oo} - B]/(a^2 \text{Cos } \lambda)^2 \tag{69}$$

and

ρ_o/ρ_{oo} is the normal shock density ratio

The streamline equations (60) and (61) reduce to

$$\frac{d\sigma}{d\zeta} = - \frac{\text{Cos } \lambda \text{ Sin } (\xi + \lambda)}{2z \text{ Cos } \xi} \tag{70}$$

$$\frac{2z}{\text{Cos}^2 \lambda} \frac{d \text{ Sin } \xi}{d\zeta} = (\lambda_\theta - 1) \text{ Sin } \xi - \frac{a \text{ Cos } \xi}{\sqrt{2z}} \text{ Cos } \lambda \, \tau_\theta$$

$$+ \left[\text{Cos } (\xi + \lambda) \text{ Cos } \lambda \frac{P_\sigma}{2z} + \text{Sin } \xi \, P_\zeta \right] \frac{2z}{\rho \bar{V}^2 \text{ Cos}^2 \lambda} \tag{71}$$

Now change independent variables from σ, ζ to $\bar{\sigma}$, $\bar{\zeta}$ where

$$\bar{\sigma} = \sigma$$

$$\bar{\zeta} = \sqrt{\psi/\rho_{oo} U_{oo} a^2 \zeta} = \sqrt{\psi/\psi_s} \tag{72}$$

Then equations (70) and (71) become

$$\bar{\zeta} \frac{d\bar{\sigma}}{d\bar{\zeta}} = \text{Tan } (\bar{\zeta} + \lambda)$$

$$\bar{\zeta} \frac{d \ (\xi + \lambda)}{d\bar{\zeta}} = \frac{G_{\bar{\sigma}}(\bar{\sigma}) - \bar{\zeta}^2 P_{1\bar{\sigma}}(\bar{\sigma}) + 2G(\bar{\sigma}) \text{ Tan } (\xi + \lambda)}{2 \left[G(\bar{\sigma}) - \bar{\zeta}^2 (P_1(\bar{\sigma}) - H(\varphi)) \right]} + \text{Tan } (\xi + \lambda) \tag{73}$$

subject to the initial values

$$\bar{\sigma} = \sigma_1 \ , \quad \xi = 1 \quad \text{at} \quad \eta = 1 \tag{74}$$

Remember that φ, and hence $H(\varphi)$ is constant along each streamline. Equations (73), subject to (74), can be solved for the streamline shapes and local values of ξ. The transformation back to physical space uses eq. (12). In the $\bar{\sigma}$, ξ system this becomes

$$\frac{\partial \eta}{\partial \bar{\zeta}} = \frac{\psi_s \ \text{Cos} \ \lambda \ \varphi_\sigma}{\rho a \sqrt{2z} \ \bar{V} \ \text{Cos} \ \xi}$$

But

$$\varphi_\sigma = \varphi_{\bar{\sigma}} - \text{Tan} \ \lambda \ \bar{\zeta} \varphi_\zeta$$

Also

$$L(\varphi) = 0 \Rightarrow \frac{\text{Cos} \ \zeta}{\text{Cos} \ \lambda} \varphi_\zeta - \frac{\text{Sin} \ (\xi + \lambda) \ \varphi_\sigma}{r \ \text{Cos}^{\tau} \ \text{Cos} \ \lambda} = 0$$

or

$$\varphi_{\bar{\sigma}} \ \text{Sin} \ (\xi + \lambda) + \bar{\zeta} \ \text{Cos} \ (\xi + \lambda) \varphi_{\bar{\zeta}} = 0$$

so that

$$\frac{\partial \eta}{\partial \bar{\zeta}} = \frac{\bar{\zeta} \varphi_{\bar{\sigma}}}{\sqrt{\rho_o / \rho_\infty} \ \text{Cos} \ (\xi + \lambda) \sqrt{\dfrac{\rho_o \bar{V}^2}{2a^2 z \rho_\infty U_\infty^2}}} \tag{75}$$

where

$$\frac{\rho_o \bar{V}^2}{2a^2 z \rho_\infty U_\infty^2} = G(\bar{\sigma}) + \bar{\zeta}^2 \left[H(\varphi) - \frac{P_1(\sigma)}{U_\infty} \right]$$

and where $\eta = 0$ at $\bar{\zeta} = 1$.

Although this has not been proved analytically, the following appears true. The solutions of eqs. (73) subject to (74), yield a result which, on insertion into (75), gives $\eta(\bar{\sigma}, \bar{\zeta})$. At least at $\bar{\zeta} = 0$, this should be a constant. Unfortunately this does not appear to be strictly true. Because of the analytic uncertainty, a computer program has been written to analyze the question numerically. Some results are shown in Table I, Because of the symmetries (eq. (64)) we need consider only one quadrant. The numerical results show a variation of about $\pm 2\%$ for the cases solved. A quasi-analytic solution is also given. This was found as follows. Two limiting solutions can be found.

$$\lim_{\rho \to \infty} \eta(0,\bar{\sigma}) = \frac{\rho_\infty}{\rho_o} \frac{\ln (1 + B)}{B} \tag{76}$$

$$\lim_{B \to 0} \eta(0,\bar{\sigma}) = \frac{\rho_\infty}{\rho_o} \Bigg/ \left[1 + \sqrt{\frac{\gamma + 5}{\gamma + 1} \frac{\rho_\infty}{\rho_o}} \right] \tag{77}$$

Arbitrarily combining these

$$\eta(0,\bar{\sigma}) = \frac{\dfrac{\rho_\infty}{\rho_o} \dfrac{\ln(1 + B)}{B}}{1 + \sqrt{\dfrac{\gamma + 5}{\gamma + 1} \dfrac{\rho_\infty}{\rho_o}}} \tag{78}$$

which agrees quite well with the numerical results (see Table I).

METHOD OF SOLUTION

The problem to be solved now consists of integrating eqs. (60), (61) and (12) subject to eq. (53) for the pressure and the associated state, entropy and isoenergy conditions. For conical flow, eqs. (62), (63) and (38) replace (60), (61), and (12).

Consider conical flow first. We begin by generating an initial estimate of the shock shape by a crude estimate based on the given body shape, angle of attack and free stream conditions. To date, the programs have thus far assumed that lateral symmetry exists although this is not necessary. This distribution is then smoothed (by repeated use of a 5-point

least squares fit) so it can be twice differentiated. Then a number of auxiliary functions can be computed and saved for later use (for example, τ, λ (eq. (3)), P_1 (eq. (54)), P_2 (eq. (55), φ_s, etc.).

Then, for a specified streamline, the entropy is known and the pressure can be found from eq. (53), using (54) and (55). Then the density and enthalpy follow from the state equation, while the local speed ($\bar{V}$) is obtained from the isoenergetic condition (eq. (53), neglecting U as discussed). Using these relations, the two differential equations (62) and (63) can be integrated to find the streamline shape and the flow direction (ξ). Repeated use of this procedure leads to a field of streamlines and values of the associated physical variables along them.

Next an interpolation routine is used to find appropriate quantities along lines of constant sigma (σ). These are required to perform the indicated integration in eq. (38a) to return to physical space.

At this point, we have found, for the specified shock, the associated flow field and (integrating to $\varphi = 0$ in eq. (38a)) the shape of the associated body (using eqs. (2) and (8)). Call the η's thus found $\eta_{BC}(\sigma)$. For the same σ using the desired body radius and the assumed shock radius, we can find from eq. (2), the associated geometric η's; call them $\eta_{BG}(\sigma)$. Compare them. If the error is small enough, we are home free. If not, the error is used as a basis to find a new estimate of the shock radius. For simplicity, the estimate has been taken as

$$r_{new} = r_{old} + SCAL\ (\eta_{BG} - \eta_{BC}) \tag{79}$$

where SCAL is a (constant) scale factor whose value has been typically 30. Larger values tend to overshoot the required corrections, lesser ones lead to slow convergence. More sophisticated iteration procedures could be used but do not appear to be necessary. The new shock radius is smoothed as before and the process repeated until convergence is satisfactory.

Finally after convergence is obtained, the flow variables along the surface streamline are found. The procedure is as described above except that, since $\psi = 0$ here, we integrate the single differential equation formed by dividing eq. (63) by (62).

For nonconical flow, the procedure is essentially the same. We solve the problem at successively increasing values of z (Figure 1). On each z = const. surface the process is exactly as for the conical case. A shock is assumed (by extrapolation from smaller z), the streamlines are found by integrating eqs. (60) and (61) one step in z (or ζ). Then the results are interpolated to constant σ and the transformation back to physical space found. The solution is iterated and when convergence is obtained the shock is interpolated to a new z and the process repeated.

For nonconical flow, one must of course have a starting procedure. For a pointed body the conical solution can be used for that purpose. For a blunted body a special starting procedure is needed.

In such a case,we still use the same equation system as before. However the procedure in the neighborhood of (though not exactly at) the stagnation point must be somewhat modified. The shock must initially have the form given in eq. (64); which we write here as

$$r^2 = 2Az/(1 + B \cos^2 \theta) \tag{80}$$

Using this form, we proceed as before. Find the auxiliary functions at the shock, integrate the differential equation (60) and (61) (being careful about $z = 0$ limits), interpolate to σ = constant and return to physical space. Now the results are to be compared with the desired body. There are only three parameters at our disposal. Two are the assumed values of A and B which describe the shock (eq. (80)). The third is the stagnation point standoff distance.

At this point there is a difficulty. If the limiting stagnation line procedure discussed previously had yielded a result (on integrating eq. (75)) which did not depend on σ at all, then all would be consistent. An iteration based on improving the values of A and B would produce the desired body shape and would yield the stagnation point standoff distance. Indeed the latter could be found separately by the method described before. Comparison of the calculated and geometric values of $\eta(\eta_{BC}, \eta_{BG})$ at two σ-stations would suffice to test the values of A and B. Unfortunately, as presently formulated, the stagnation line result is not quite constant (Figure 2) and the variation appears to be too large for comfort in the subsequent calculations. Hence an alternate procedure has been written into the computer program. Using the assumed shock (eq. (80)), the solution at two z-stations is found. The resulting body is tested in an average way to find both the values of A and B and the stagnation standoff distance. At the time of writing this report, it is too early to tell whether the procedure is acceptable.

NUMERICAL RESULTS

Limiting solutions along the stagnation line have been found by integrating eqs. (72) and then (75). Typical results for the standoff distance are shown in Table I. The r.m.s. value of the standoff distance is given for each case gogether with r.m.s. deviation from that value. The results are gratifying in that they are relatively uniform and

TABLE I

STAGNATION POINT CASES

ρ_o/ρ_∞	B (eq. (64))	$\eta(0,\sigma)$ (eq. (78)) (Approx.)	$\eta(0,\sigma)_{RMS}$ (Calculated)	$\Delta_{RMS}\eta(0,\sigma)$
6	1	.06931	.06669	.001169
20	1	.02539	.02462	.0003280
50	1	.01126	.01098	.0001195
200	1	.003107	.003046	.00002968
6	0	.01000	.009985	.0000
6	1	.06931	.06669	.001169
6	2	.05493	.05008	.001610
6	4	.04021	.03349	.001963

Note: For all calculations $\gamma = 1.4$, but the normal shock density ratio is assumed to be separately varied as shown.

close to the approximate result from eq. (78). They are disappointing mainly in that they are not exactly uniform as they must of course be physically.

For conical flow, a number of cases have been run (Table II). The cases chosen were ones for which other detailed calculations were available in the literature. The program provides the details of the flow variables and physical coordinates in the field on σ = const lines at equal intervals in ψ, as well as at the body surface. It also computes the streamline shapes and records the final shock shape. For the first two cases in the table, the computed values of surface pressure and shock angle agreed with the values given in ref. (6) to about 1%. Figures 2 through 6 show the surface pressures and, for some cases, the shock shape and streamlines for the remaining cases listed in Table II. It should be noted that in some of the figures, the ordinate scale does not begin at zero. Also for those cases where the broken lines disappear, they fall on the corresponding solid lines.

TABLE II

CONICAL FLOW CASES

M_∞,	angle of attack (deg.)	cone shape
4.25	0	$12\frac{1}{2}°$ half angle, circular
10.00	0	$12\frac{1}{2}°$ half angle, circular
4.25	8.24	$12\frac{1}{2}°$ half angle, circular
3.53	10	20° half angle, circular
6	0	21.3° x 12.9° half angle, elliptic
5.8	0	11.8° x 6° half angle, elliptic
5.8	4*	11.8° x 6° half angle, elliptic
5.8	8*	11.8° x 6° half angle, elliptic
5.8	4**	6° x 11.8° half angle, elliptic
5.8	6**	6° x 11.8° half angle, elliptic

* along major axis
** along minor axis

Note (for all cases):

γ (ratio of specific heats)	=	1.4
step size (in $\bar{\sigma}$)	=	10°
step size (in $\bar{\psi}$)	=	.05 of its value at shock
SCAL (eq. (79))	=	.30

For the circular cone cases shown in Figure 2, comparison is made with the results of Jones (ref. 7). The pressures are also in good agreement (not shown) with Rainbird's experiments (ref. 8). For the cone of Figure 3, the experimental pressures of Holt and Blackie (ref. 9) agree well with the analytic curves presented. The theoretical results of Holt and Ndefo (ref. 10) also agree well. In the case of the ellipse in Figure 4,

Ferri's results (ref. 11) generally agree, although not as well as in the previous figures. Finally for the cone in Figures 5 and 6, the results of Chapkis (ref. 12) are in excellent agreement with the theoretical curves, falling generally closer to the results by the method of lines (ref. 13). In general the agreement of the surface pressures is quite satisfactory.

For the cases shown, the shock shapes (Figs. 2, 3, 4, 6) and streamlines (Figs. 2-4) are in very good agreement with other calculations.

Finally, the total running time on a UNIVAC 1108 for the ten cases listed in Table II was about 80 seconds. The number of iterations required for convergence of a solution was typically four or five.

CONCLUDING REMARKS

The analysis presented depends for its utility on the quality of the approximate pressure relation obtained from the lateral momentum equation, and on the convergence rate from the initial estimated shock shape to the final one. Earlier results (refs. 1, 2) for axisymmetric flow showed good pressure predictions as do the present conical flow cases. The main reason for pursuing the conical program was to resolve the second question, namely the ability to get rapid convergence. This has in fact worked out well. For example, for the 2:1 ellipse shown in Figures 5 and 6, the number of iterations required varied between 3 and 5 for the various angles of attack.

The theoretical results presented for conical flow are especially gratifying in that they represent an application where the thin shock layer assumption is somewhat strained. The stream Mach number is low enough and the cone slender enough that the shock layer thickness is greater than the cone thickness in some cases.

Experience with the conical program together with some preliminary results (not shown) with a program for the general blunt body give confidence that an efficient, accurate, general method can be developed.

REFERENCES

1. Maslen, S. H.: Inviscid Hypersonic Flow past Smooth Symmetric Bodies. AIAA J., Vol. 2, pp. 1055-1061, 1964.

2. Jackson, S. K.: The Viscous-Inviscid Hypersonic Flow of a Perfect Gas over Smooth Symmetric Bodies. Ph.D. thesis, U. of Colorado, 1966. Available from University Microfilms, Ann Arbor.

3. Perini, L. L. and Melnik, W. L.: Nonequilibrium Flow Past Smooth Symmetric Bodies, J. Space. Rockets, Vol. 5, N. 3, pp. 308-312, March 1968.

4. Olstad, W. B.: Nongray Radiating Flow about Smooth Symmetric Bodies. AIAA J., Vol. 9, N. 1, pp. 122-130, January 1971.

5. Grose, W. L.: A Thin Shock Layer Solution for Nonequilibrium Inviscid Hypersonic Flows in Earth, Martian, and Venusian Atmospheres. NASA TN D-6529, 1971.

6. Ames Research Staff: Equations, Tables and Charts for Compressible Flow, NACA TR 1135, 1953.

7. Jones, D. J.: Numerical Solutions of the Flow Field for Conical Bodies in a Supersonic Stream, Aero Rept. LR-507, National Research Council (Canada), July 1968.

8. Rainbird, W. J.: Turbulent Boundary Layer Growth and Separation on a Yawed $12\frac{1}{2}^\circ$ Cone at Mach Numbers 1.8 and 4.25. AIAA Paper No. 68-9A, Jan. 1968.

9. Holt, M. and Blackie, J.: Experiments on Circular Cones at Yaw in Supersonic Flow. J. Aero Sci., Vol. 23, N. 10, pp. 931-936, Oct. 1956.

10. Holt, M. and Ndefo, D. E.: A Numerical Method for Calculating Steady Unsymmetrical Supersonic Flow Past Cones. J. Comp. Phys., Vol. 5, N. 3, pp. 463-486, June 1970.

11. Ferri, A.: Review of Recent Developments in Hypersonic Flow. Adv. Aero. Sci., Vol. 2, Pergamon Press, 1959.

12. Chapkis, R. L.: Hypersonic Flow over an Elliptic Cone: Theory and Experiment. J. Aero. Sci., Vol. 26, N. 11, pp. 844-854, Nov. 1961.

13. South, J. C. and Klunker, E. B.: Methods for Calculating Nonlinear Conical Flows. Presented at NASA Symposium on Analytic Methods in Aircraft Aerodynamics, Ames Research Center, Oct. 1969. (Available in NASA SP-228, 1970)

14. Stocker, R. M. and Mauger, F. E.: Supersonic Flow past Cones of General Cross-Section, J. Fluid Mech., Vol. 13, pp. 383-399, 1962.

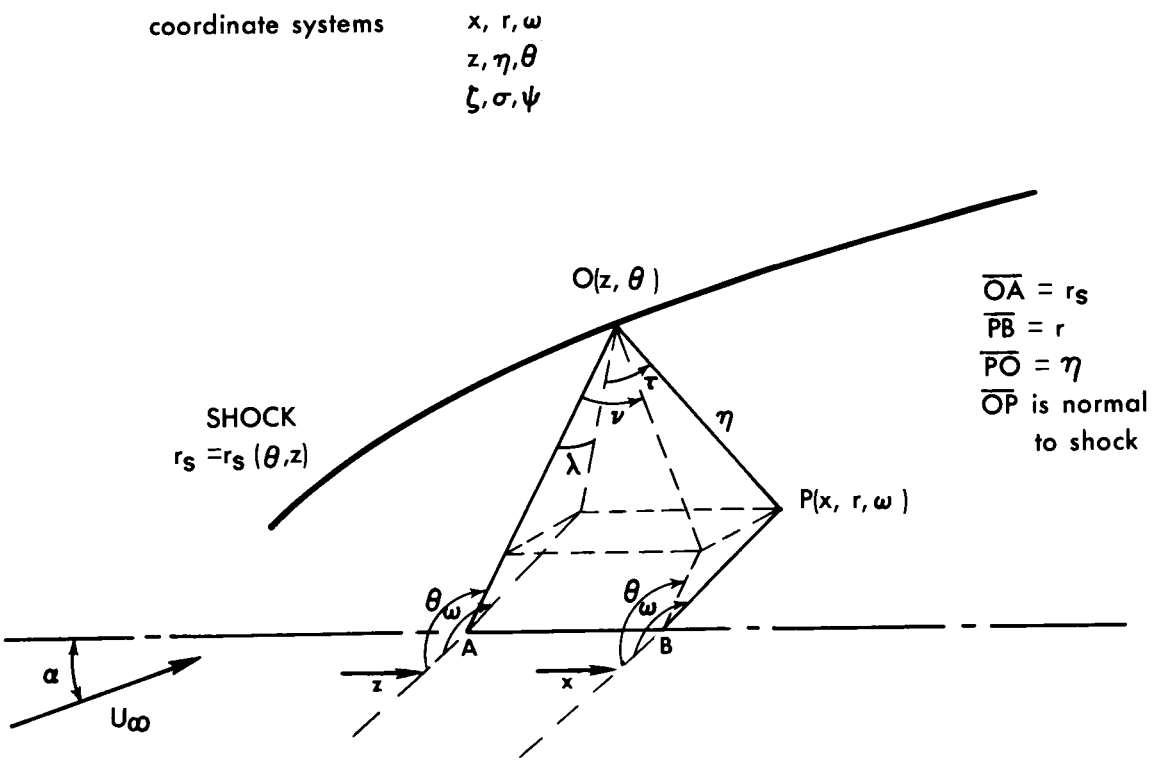

Fig. 1 - Coordinate systems

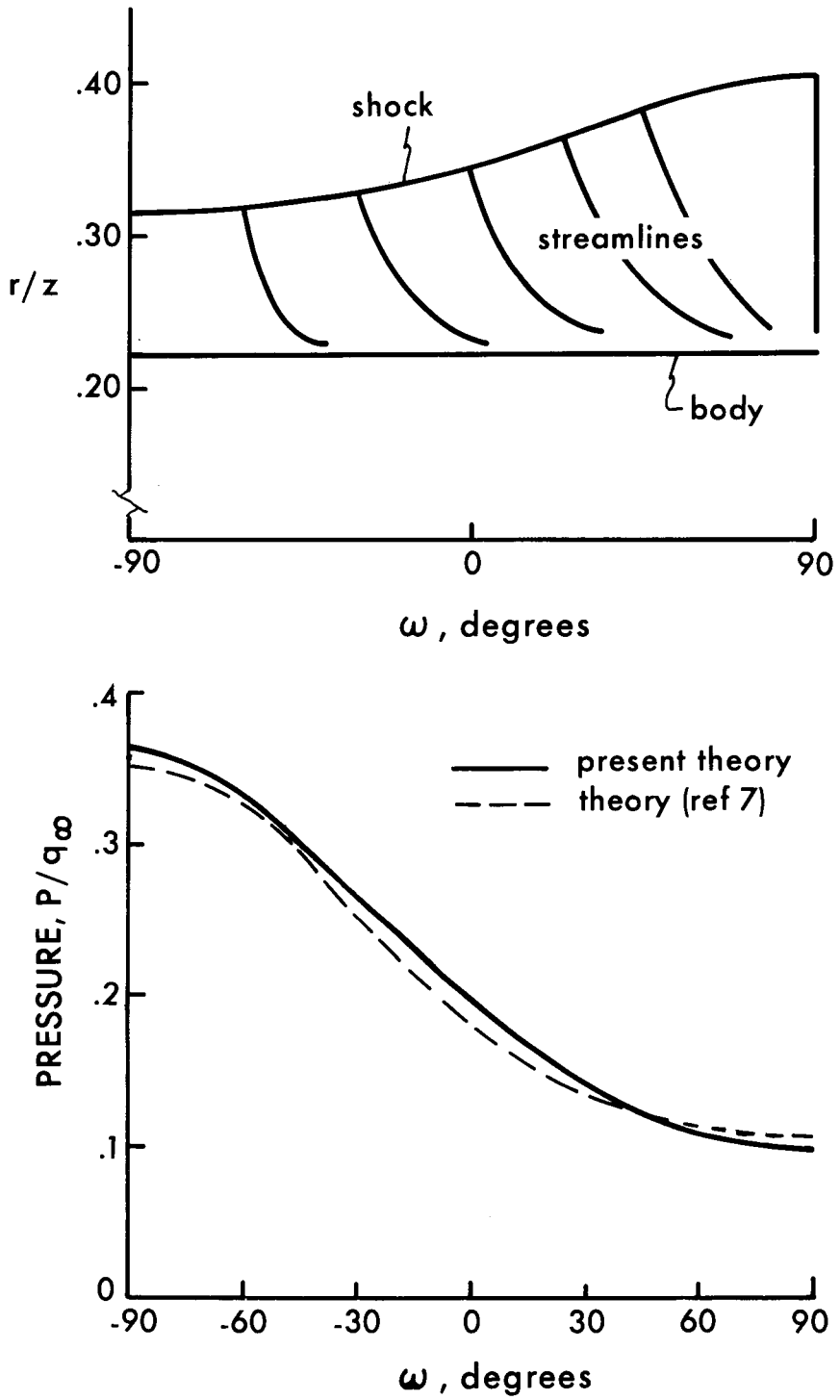

Fig. 2 - Surface pressure, shock shape and streamlines for circular cone of half-angle 12.5°, at M = 4.25 and α = 8.24°

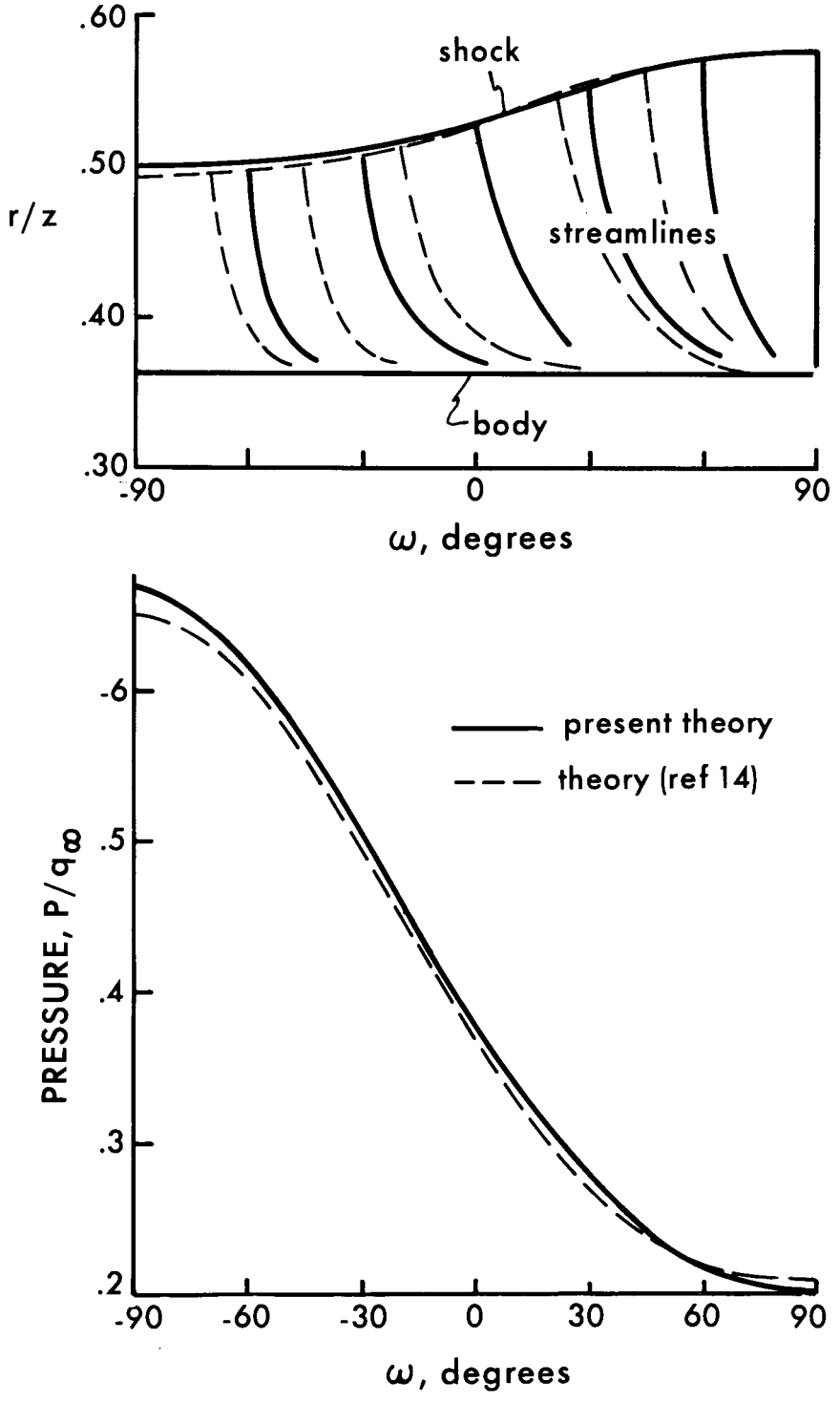

Fig. 3 - Surface pressure, shock shape and streamlines for circular cone of half angle 20° at M = 3.53, α = 10°

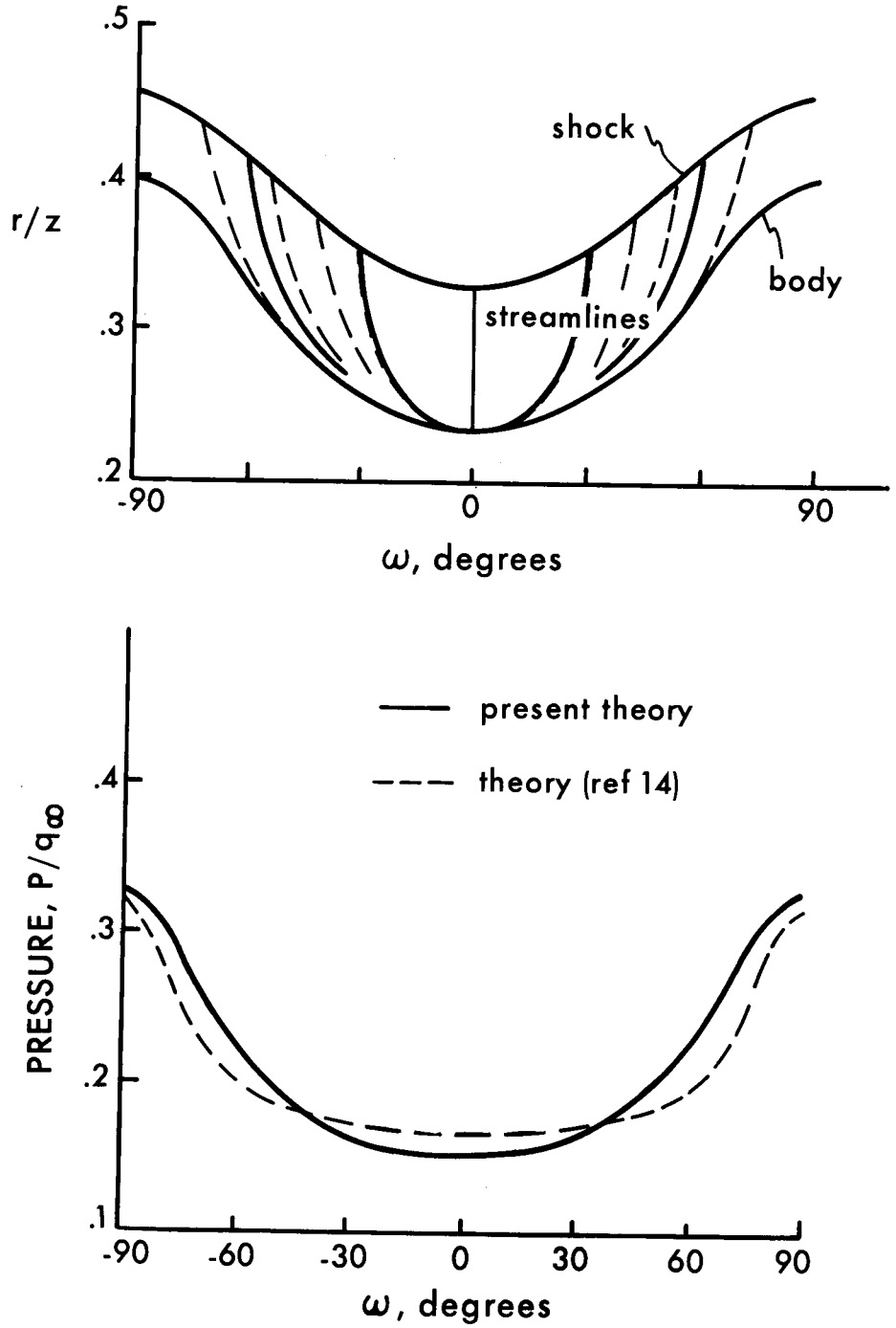

Fig. 4 - Surface pressure, shock shape and streamlines for 12.9° x 21.3° elliptic cone at M = 6.0, α = 0°

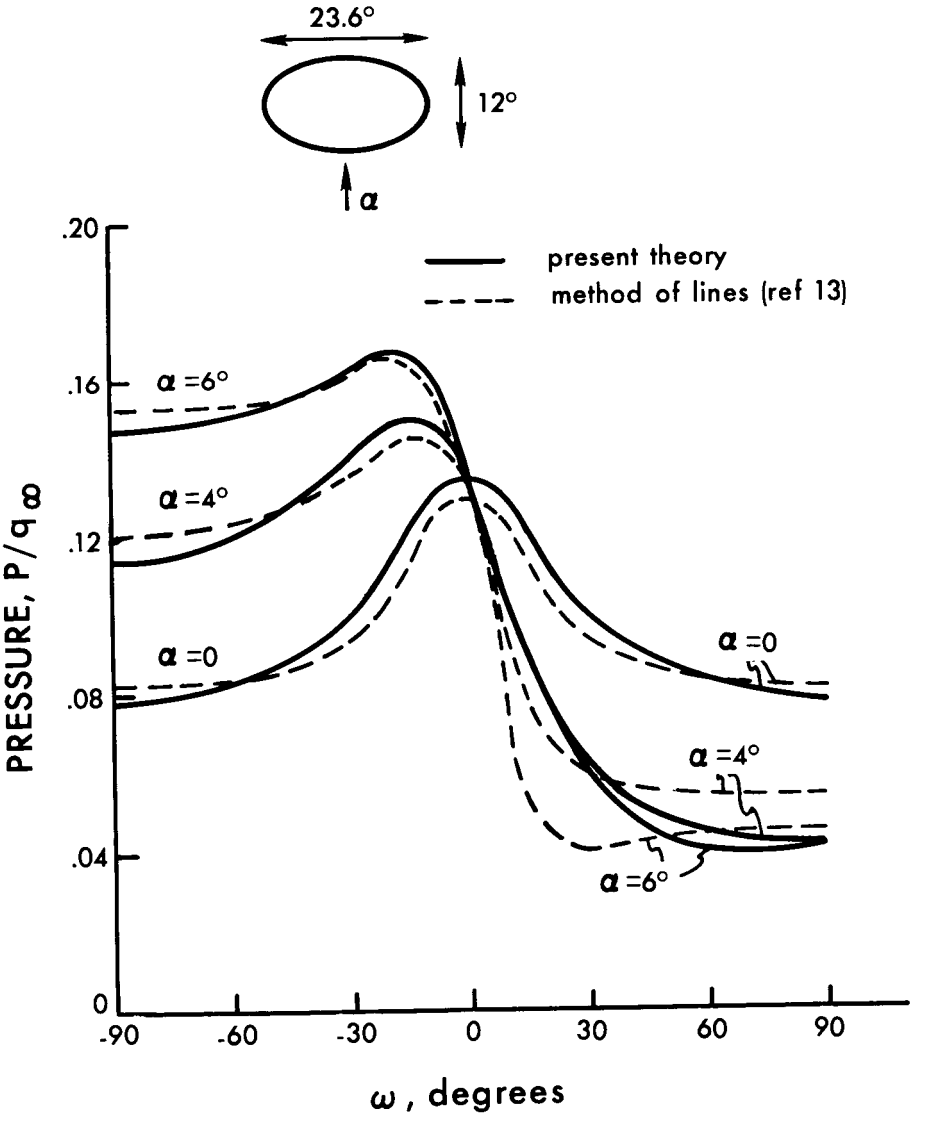

Fig. 5 - Surface pressure distribution on elliptic cone at M = 5.8

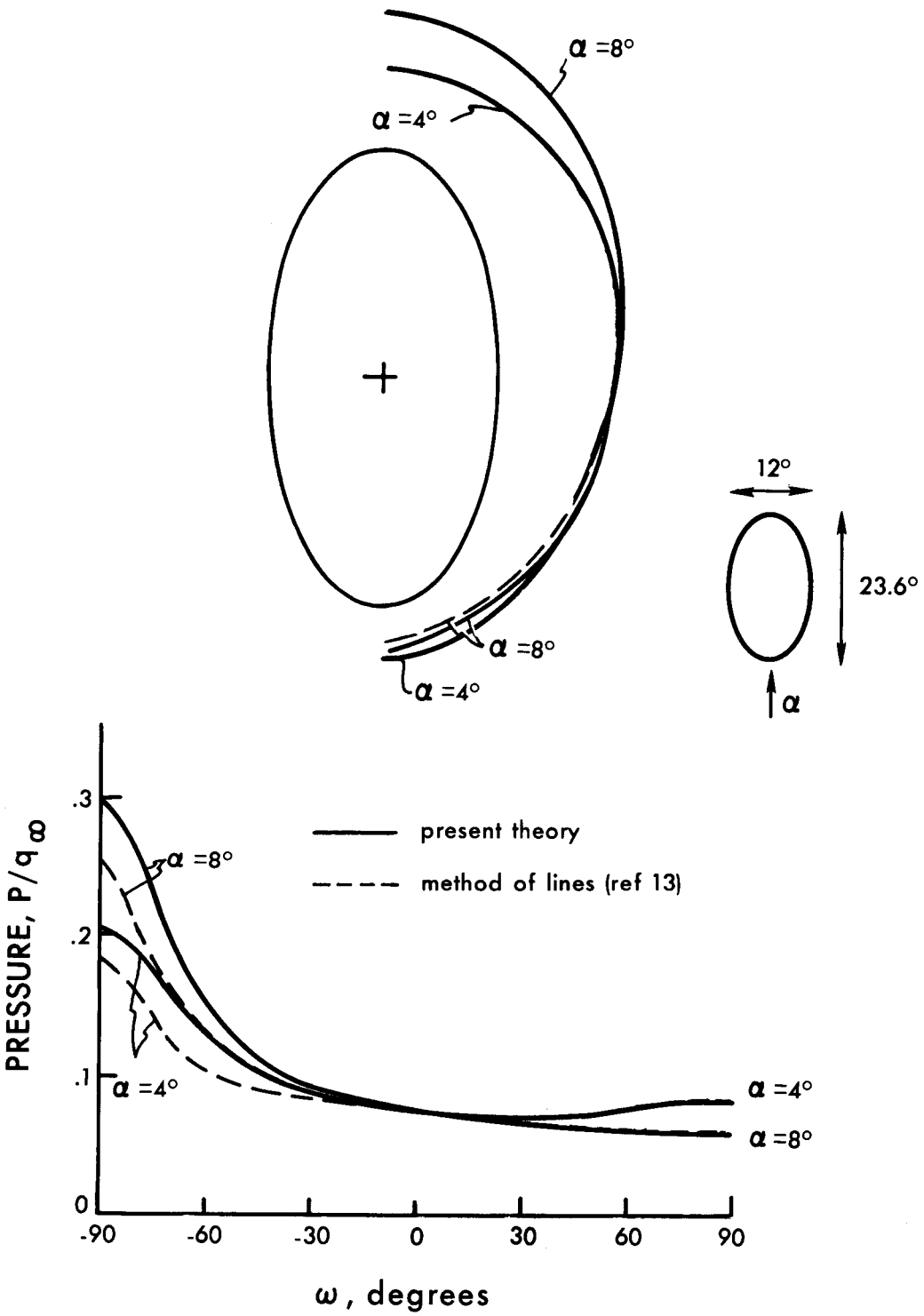

Fig. 6 - Pressure distribution and shock shapes for elliptic cone at M = 5.8